Journal of Alloys and Compounds 538 (2012) 66–72

Contents lists available at SciVerse ScienceDirect

Journal of Alloys and Compounds

journal homepage: www.elsevier.com/locate/jalcom

Structural, electrical and thermal properties of borosilicate glass–alumina composites

M.M.R.A. Lima [a], R.C.C. Monteiro [a,*], M.P.F. Graça [b], M.G. Ferreira da Silva [c]

[a] Department of Materials Science, CENIMAT/I3N, Faculty of Sciences and Technology, Universidade Nova de Lisboa, 2829-516 Caparica, Portugal
[b] Department of Physics, FSCOSD/I3N, Universidade de Aveiro, Campus Universitário de Santiago, 3800-193 Aveiro, Portugal
[c] Department of Glass and Ceramic Engineering, CICECO, Universidade de Aveiro, Campus Universitário de Santiago, 3800-193 Aveiro, Portugal

ARTICLE INFO

Article history:
Received 27 February 2012
Received in revised form 3 May 2012
Accepted 6 May 2012
Available online 5 June 2012

Keywords:
Sintering
Glass/ceramic composites
Dielectric properties
Thermal expansion
XRD
SEM

ABSTRACT

Borosilicate glass–alumina composites with $(1-x)$ Glass + x Al_2O_3 (x = 0, 5, 10, 25 vol.%) were prepared and the effect of Al_2O_3 addition on the structural, electrical and thermal characteristics was investigated. XRD patterns revealed the presence of cristobalite (SiO_2) in sintered borosilicate glass and that the addition of Al_2O_3 hinders cristobalite formation. This behavior is due to the diffusion of some Al^{3+} ions from alumina to glass, which leads to changes in glass structure and composition as identified by SEM/EDS. Cristobalite was undetected in composites containing 10% Al_2O_3 that attained the lowest thermal expansion coefficient value ($\sim 4.6 \times 10^{-6}\ °C^{-1}$). Conductivity (dc and ac) increased with the amount of Al^{3+} ions present in the glass structure as modifiers and formers. Dielectric constant values, in the range 5.0–7.2, increased with Al_2O_3 addition and the values of loss $\tan\delta$ ($1.5–2.1 \times 10^{-2}$) indicate that these materials are good insulators.

1. Introduction

The idea of combining two or more different components to produce new materials with unique properties has been used for many years. Glass–alumina composites, namely borosilicate glass with alumina, present a large potential as substrate materials for integrated circuits (IC) because they can be densified at low temperatures and present the required electrical and thermal characteristics [1–3].

Borosilicate glasses constitute a family of glasses with a large number of applications, particularly due to their low coefficient of thermal expansion, similar to that of silicon ($3.4 \times 10^{-6}\ °C^{-1}$) [1], high electrical resistance (10^{11}–$10^{13}\ \Omega\,m$) [4], low dielectric constant (4.8 at 1 MHz) [5] and to their high resistance to chemical attack [3,5,6]. Due to their low softening temperature (800 °C) [7], some borosilicate glasses in the form of powders have particular interest for their use in the production of sintered glasses with controlled porosity [8] and for their application in the manufacture of sintered glass–ceramic composites [3,7,9–14]. If these composites present adequate properties (e.g. low dielectric constant, high electric resistivity, coefficient of thermal expansion matching that of IC chips, good chemical and environmental stability and sufficient mechanical strength) they can be used as substrates for microelectronic packaging [5,15–19].

Alumina (Al_2O_3) has been the dominant ceramic substrate material due to its particular properties such as moderate strength and thermal conductivity as well as its relative low cost [20,21]. However, sintering of pure Al_2O_3 requires high temperatures (~1500 °C) [15]. The association of Al_2O_3 to a glass-forming system contributes usually to the reduction of the sintering temperatures [22]. If a suitable glass composition is selected, the composite materials can have controlled closed porosity and the dielectric constant, thermal expansion and hermeticity required for high performance microelectronic substrates [5,20]. Furthermore, the reduction of the sintering temperature through the use of glass allows co-firing with low resistance conductors, such as gold and copper [5].

A selection of the properties of borosilicate glass and alumina, considered individually as potential substrate materials, is presented in Table 1, taking into account data reported in literature [4,7,16,19,20,23,24]. The properties of borosilicate glass–Al_2O_3 composites depend on the properties of the constituents, on their relative amounts and on the processing conditions that can determine not only the microstructure of the final composite material but also the structure and composition of the residual glass.

In some cases, devitrification of the borosilicate glass may happen during firing, with cristobalite (SiO_2) precipitation, which makes difficult to obtain the required properties as cristobalite affects particularly the thermal expansion of the composites [5]. Also, cristobalite precipitation within the glass matrix makes the composite more difficult to densify because it is more viscous than

* Corresponding author. Tel.: +351 212948564; fax: +351 212957810.
E-mail address: rcm@fct.unl.pt (R.C.C. Monteiro).

0925-8388/$ - see front matter © 2012 Elsevier B.V. All rights reserved.
http://dx.doi.org/10.1016/j.jallcom.2012.05.024

Table 1
Selected properties of borosilicate glass and alumina compiled from literature [4,7,16,19,20,23,24].

Material	Dielectric constant (at 1 MHz)	Flexural strength (MPa)	Coefficient of thermal expansion (20–300 °C) (10^{-6} K^{-1})	Thermal conductivity (W m^{-1} K^{-1})	Process temperature (°C)
Borosilicate glass	4.8	70	3.3	2	800
Alumina	9.2–9.8	250–397	5.5–7.1	21	1500

Table 2
Compositions and characteristics of borosilicate glass and Al_2O_3 powders used in the present work [30].

	Composition (wt.%)								ρ[a] (g/cm^3)	S[a] (m^2/g)	d_{50}[a] (μm)
	SiO_2	B_2O_3	Al_2O_3	Na_2O	K_2O	CaO	Fe_2O_3	MgO			
Glass	79.78	12.3	2.33	4.8	0.77	–	–	–	2.23	3.82	10.8
Al_2O_3	0.03	–	99.78	0.06	–	0.01	0.02	0.03	3.91	12.53	2.5

[a] ρ – Density; S – Specific surface area; d_{50} – Mean particle size.

with a single-phase glassy matrix [5,25]. Several ceramic fillers have been added to the borosilicate glass matrix in order to suppress cristobalite precipitation [6,7,25,26], with the aim of improving the dimensional stability and to help tailor the final properties of the composites [3,7].

The present study follows an early work [27,28] where the densification and crystallization processes of a borosilicate glass [27] and a borosilicate glass-25 vol.% Al_2O_3 composite [28] were investigated. Borosilicate glass matrix composites with different proportions of Al_2O_3 inclusions were prepared by a powder technology and sintering route. The objective of this study was to investigate the effects of composition and firing temperature on the structural, microstructural, electrical and thermal characteristics exhibited by the sintered composites.

2. Experimental procedure

2.1. Materials and processing

A borosilicate glass powder (Corning France, code 658909) and Al_2O_3 powder (SG16 from Alcoa, UK), with the compositions and characteristics specified in Table 2, were used as starting materials in this study. Compositions of the starting materials were specified by the suppliers. The density of the powders, measured with a helium pycnometer, the specific surface area, measured by the nitrogen-BET method and the mean particle size, measured by laser diffraction, were determined by one of the authors in a previous work [29].

Powder mixtures of both starting materials were prepared, where the Al_2O_3 content was 0, 5, 10 and 25 vol.%. The powders were intensively dry mixed for 2 h in a laboratory powder mixer (turbula WAB, T2F). Powder compacts with 13 mm diameter and 3–4 mm height were obtained by uniaxial pressing at 74 MPa.

The different composition samples (named as G, G-5A, G-10A and G-25A, according to the Al_2O_3 addition) were heated in an electrical tubular furnace, in air, at a heating rate of 10 °C min^{-1} up to 800 and 1000 °C, and maintained for 3 h at the selected temperature. After this, the furnace was switched off and the specimens were allowed to cool down inside the furnace. The sintering temperatures of the borosilicate glass–Al_2O_3 composites were selected taking into account the thermal characteristics of the borosilicate glass, specifically the glass transition temperature (530 °C) and the dilatometric softening temperature (630 °C) that had been determined by differential thermal analysis and dilatometry, respectively, as reported in a previous work [30]. In order to determine the volume fraction of open porosity, the sintered samples were immersed into distilled water and the open pores were filled with boiling water for 30 min. Bulk densities of the sintered composites were determined by the Archimedes displacement method, using water at room temperature. The theoretical density of the composites was calculated by the rule of mixtures taking into account the glass and alumina densities [29], which were respectively, 2.23 and 3.91 g cm^{-3} (*cf.* Table 2). At least three powder compacts of each composition were sintered at the selected temperature and the mean values of the bulk density and open porosity of the sintered composite samples were determined.

2.2. Structural and microstructural characterization

The crystalline phases present in sintered composites were identified by X-ray diffraction (XRD), performed in a Rigaku diffractometer (model DMAX III-C3 kW) at room temperature with Cu kα radiation. A scanning electron microscope, Zeiss (model DSM 962), attached to an energy dispersive spectroscopy unit (SEM–EDS), was used to observe the microstructure and to carry out X-ray chemical microanalysis of the sintered composites.

2.3. Thermal expansion characterization

Prismatic powder compacts (≈12 mm height, 4 × 5 mm cross section) were prepared from the different binary glass–Al_2O_3 compositions by uniaxial pressing and sintered under the same conditions as indicated in Section 2.1. The sintered prismatic samples were heated at 5 °C min^{-1} from room temperature up to 300 °C in a horizontal dilatometer (Adamel Lhomargy, DI24) in order to determine the thermal expansion coefficient of the sintered composites.

2.4. Electrical and dielectric characterization

For the electrical measurements the opposite sides of cylindrical samples, with a thickness of 1 mm approximately, were painted with silver paste. The dc conductivity (σ_{dc}) was measured with a Keithley electrometer, model 617, as a function of temperature, in the range 280–360 K. During the measurements, the samples were in a helium atmosphere to improve the heat transfer and eliminate moisture. The Arrhenius expression (Eq. (1)) was used to fit the temperature dependence of σ_{dc} [31–34],

$$\sigma_{dc} = \sigma_0 \exp\left(\frac{E_{a(dc)}}{k_B T}\right) \quad (1)$$

where σ_0 is a pre-exponential factor, $E_{a(dc)}$ the dc activation energy, k_B the Boltzmann constant and T the temperature.

The ac conductivity (σ_{ac}) measurements were performed with an Ardeen Hagerling Automatic Capacitance Bridge, model 2500, operating at 1 kHz, in the temperature range of 200–360 K, measuring the capacitance (C) and the conductance (G) of the sample. The ac conductivity, σ_{ac}, was calculated using relation (2) [31,35]:

$$\sigma_{ac} = \varepsilon'' \omega \varepsilon_0 \quad (2)$$

where ω is the angular frequency, ε_0 is the dielectric permittivity of free space (8.854×10^{-12} F/m) and ε'' is the imaginary part of the dielectric permittivity obtained through the G values. The real part of the dielectric permittivity (ε) was obtained through the C values.

The frequency dependence of the complex permittivity, $\varepsilon^* = \varepsilon + j\varepsilon''$, was measured at room temperature, in the frequency range from 100 Hz to 100 kHz using a SR850 DSP Lock-In Amplifier, in the typical lock-in configuration, measuring the "in-phase" and "out-of-phase" components of the output signal [31,35].

3. Results and discussion

3.1. Sintering, microstructural and structural behavior

The effect of Al_2O_3 content and sintering temperature on the relative density (ρ_r) and open porosity of the composites is illustrated in Figs. 1 and 2, respectively. Considering the data presented in Fig. 1, it is observed that the relative density of the composites decreases for volume fractions of filler higher than 5% and that the increase in sintering temperature has a beneficial effect on the final density of the composites. With the exception of sample G-25A sintered at 800 °C, all the composites exhibited a relative density ⩾92% (total porosity ⩽8%), and the highest sintered density

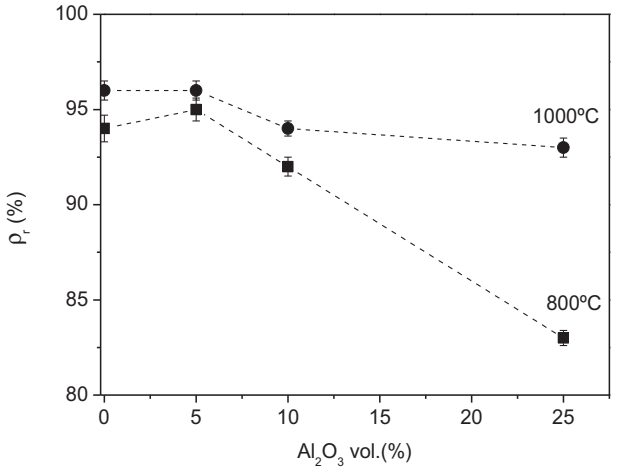

Fig. 1. Effect of Al_2O_3 content on the relative density of the sintered composites.

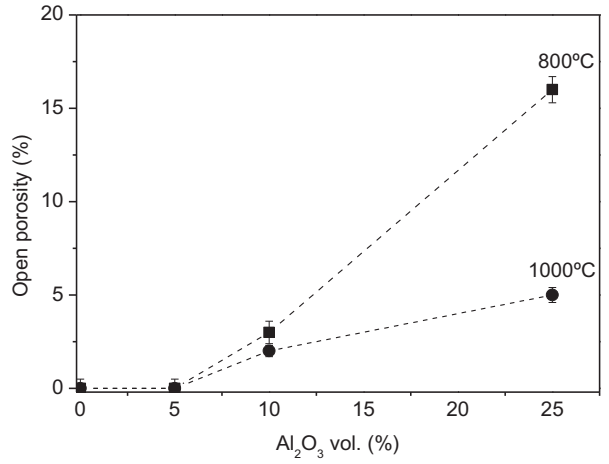

Fig. 2. Effect of Al_2O_3 content on the open porosity of the sintered composites.

(~96%) was achieved by G and G-5A samples when heated at 1000 °C. From Fig. 2 it is verified that, after sintering at any of the selected temperatures, only closed porosity was present both in G and G-5A samples, as the measured value for open porosity is 0%. Composites with 10 vol.% Al_2O_3 presented a lower open porosity than composites with 25 vol.% Al_2O_3. For these last ones, an open porosity of about 15% still remained after sintering at 800 °C, and of about 5% after sintering at 1000 °C, meaning that a higher sintering temperature is necessary for the densification of the composites with 25% filler volume fraction [28], and therefore to guarantee the hermeticity of the composites.

The results presented in Figs. 1 and 2 show that there are two factors affecting the bulk density and apparent porosity of the glass–ceramic composites, which are the filler content in the composite material and/or the sintering temperature. The increase in Al_2O_3 addition contributed to hinder the densification and, for all compositions, higher density was observed after sintering at the highest temperature.

In previous works related with the sintering of glasses and of glass matrix composites containing rigid inclusions [36–39], it has been shown that the predominant mechanism of densification is the viscous flow of the glass. The sinterability of the composites decreases as the fraction of ceramic particles increases and it is promoted by the rising in temperature that enhances the glass viscous flow [39]. Accordingly, the densification results obtained in the present study demonstrate that when the composite samples

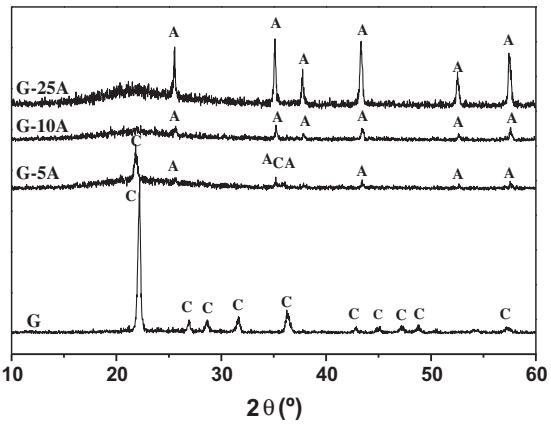

Fig. 3. XRD patterns for glass and glass–Al_2O_3 composites (G–*x*A), sintered for 3 h at 800 °C (*x* = 0, 5, 10, 25 vol.%; C – Cristobalite; A – Alumina).

were treated at the highest selected temperature, the borosilicate is much more softened and viscous flow occurs more easily because the glass–Al_2O_3 composites are better densified. The optimum sintering temperature, i.e., the temperature at which the bulk density of a sintered composite sample reaches its highest value, depends on the amount of glass, and it should not be exceeded otherwise the increase of the closed pores and warping of the samples may be observed.

The structural changes that occurred during the sintering process were evaluated by XRD analysis. Fig. 3 presents the XRD patterns obtained for all composites sintered at 800 °C for 3 h. The XRD pattern for sintered glass (G) revealed that the crystallization of the glass occurred during the sintering process, with formation of cristobalite. This phase was also identified by XRD in the case of composites containing 5 vol.% Al_2O_3 (G-5A), although with less intense diffraction peaks. The presence of cristobalite was not identified in the remaining composites (G-10A and G-25A), since the XRD results showed that alumina was the single crystalline phase. Similarly, after sintering at 1000 °C, cristobalite formation was detected in G and G-5A samples, but in composites with higher Al_2O_3 content no cristobalite was detected.

Devitrification of the glass during sintering with precipitation of cristobalite is undesirable [40–43], because this phase has a very high coefficient of thermal expansion, about 50×10^{-6} °C^{-1} [40], and it causes the appearance of microcracks within the samples [29], decreasing their final mechanical strength. The effect of Al_2O_3 addition to borosilicate glass on cristobalite formation has already been investigated by different authors [7,41–43]. It has been found that with an addition of Al_2O_3 greater than a critical value, cristobalite formation can be completely inhibited, and that the critical Al_2O_3 content decreases with decreasing Al_2O_3 particle size and with increasing sintering temperature [41,43].

Fig. 4 shows the SEM micrographs of samples G, G-5A and G-10A after sintering at 800 °C for 3 h. SEM micrograph of sample G (Fig. 4a) exhibits a dense microstructure with a few number of spherical closed pores, having a mean size of about 5 μm. Large zones with a smooth fracture surface, which is a typical feature of glass, together with some rough surface zones, due to the presence of a crystallized phase, can be observed in Fig. 4a. Taking into account the XRD results for sintered G sample, the crystallized phase corresponds to cristobalite, formed during the sintering process. SEM micrograph of G-5A (see Fig. 4b) shows also a well-densified microstructure with some closed pores having an irregular shape, and some small crystals dispersed in the glass matrix. A less dense microstructure was observed for G-10A (Fig. 4c), where some interconnected porosity was still present, and where some

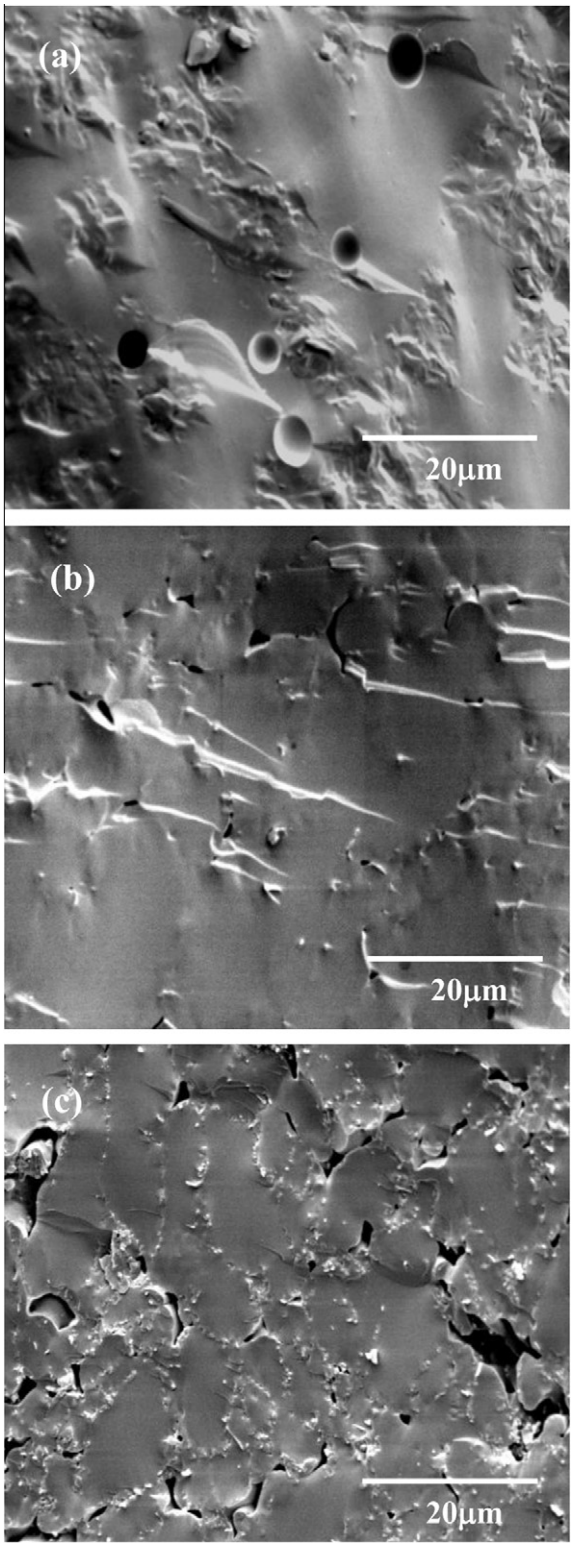

Fig. 4. SEM micrographs of samples G (a), G-5A (b) and G-10 (c) sintered at 800 °C.

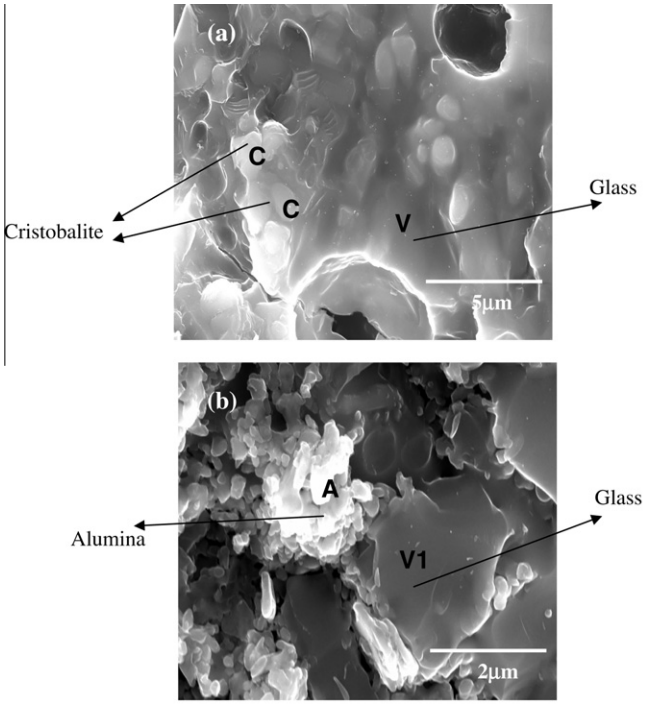

Fig. 5. SEM micrographs of samples G (a) and G-10 (b) sintered at 800 °C.

Table 3
Average elemental chemical analysis (at.%) of the glass (V) and cristobalite (C) regions, and of the glass (V1) and alumina (A) regions, identified in the microstructures of samples G and G-10A, respectively, sintered at 800 °C for 3 h (see Fig. 5), as determined by SEM–EDS.

Element	V	C	V1	A
Si	31.27 ± 6.09	25.79 ± 3.84	25.20 ± 3.94	16.02 ± 2.34
Al	1.79 ± 0.46	1.50 ± 0.49	16.03 ± 3.46	24.34 ± 5.35
Na	3.29 ± 0.89	1.11 ± 0.78	1.72 ± 0.58	2.15 ± 0.66
K	0.19 ± 0.10	–	0.19 ± 0.10	–
O	63.32 ± 10.38	80.69 ± 9.53	56.86 ± 9.53	57.48 ± 9.41

small crystals were distributed along the boundaries of large glass areas that are bond to each other due to viscous flow of the glass.

According to XRD results (Fig. 3), the amount of cristobalite precipitated in the borosilicate glass matrix of the composites decreased with Al_2O_3 addition, and in composites with an Al_2O_3 content $\geqslant$10 vol.% the presence of cristobalite was not detected. A possible explanation for this was obtained correlating these results with those from SEM/EDS analysis of the composites, by performing a more detailed observation of the microstructures at higher magnification (Fig. 5) and elemental chemical microanalysis of specific zones in the microstructures (Table 3). SEM micrograph for sample G (Fig. 5a) clearly reveals the presence of cristobalite crystals within the glass and the appearance of a microcrack that can be attributed to the high coefficient of thermal expansion of cristobalite as referred above. Spherical closed pores inside the glass matrix are observed, indicating that under such firing conditions (800 °C for 3 h) the final sintering stage has been attained for sample G. SEM micrograph for sample G-10A (Fig. 5b) shows clusters of small alumina crystals situated at the boundaries of the amorphous phase areas and the presence of irregular interconnected pores. It appears that the Al_2O_3 clusters can favor the existence of the residual pores and reduce the attainable densification.

The results of the average elemental chemical microanalysis of the glass (V) and cristobalite (C) regions and of the glass region (V1) and alumina clusters (A), identified in the microstructures (Fig. 5) and determined by energy dispersive spectroscopy (EDS), are summarized in Table 3. The results of EDS analysis of such very small (~2 μm) regions can only be considered as qualitative because the effects of EDS interaction volumes (which can be of the order of 5 μm) must be taken into account [44]. In spite of this, the data indicate that the amount of Al is higher in V1 than in V, that the amount of Na is higher in A than in V1, and that an

appreciable amount of Si and Na is present in A. These results suggest that, in the Al_2O_3 containing composite, partial dissolution of the dispersed crystalline particles into the glass phase occurred during the firing process, with Al^{3+} diffusion from alumina to the glass structure, and Si^{4+} and Na^+ diffusion from the glass to alumina. These results are in good agreement with those obtained by Jean and Gupta [41,42] on the study of the kinetics of the reaction between Al_2O_3 and a borosilicate glass. According to these authors, the inhibition of cristobalite crystallization was attributed to the dissolution of Al_2O_3 (an intermediate oxide) by the glass with corresponding Si^{4+} depletion in the glass network and substitution for the coupling of Al^{3+} and Na^+. The dissolution of Al_2O_3 and the increase of Al^{3+} concentration in the glass causes the Na^+ segregation from the borosilicate, and thus a Na^+ and Al^{3+} layer is formed around the Al_2O_3 particles [41]. The crystallization of the glass in the presence of Al_2O_3 does not occur because the kinetics of diffusion of the alkaline ions in the glass is more favorable than the kinetics of the cristobalite crystallization [41,42].

3.2. Thermal expansion characteristics

Because the deleterious effect of cristobalite formation on the final thermal characteristics of glass–alumina composites, the determination of the coefficient of thermal expansion of the various prepared composites appears of primordial interest. Table 4 shows the coefficient of thermal expansion (CET) for the different samples sintered at 800 and 1000 °C. It is verified that sample G sintered at 800 °C exhibits the highest CET value, followed by sample G sintered at 1000 °C, which shows the second highest value. Sintered G samples show higher CET values than sintered G-A composite samples due to the presence of larger amounts of cristobalite, as it is observed through the XRD patterns shown in Fig. 3. CET for borosilicate glass is 3.3×10^{-6} °C^{-1} [4] (Table 1), while CET for cristobalite is 50×10^{-6} °C^{-1} [40].

Considering the effect of alumina addition on the CET of the sintered composites, from Table 4 it is verified that CET values decrease with Al_2O_3 addition, reaching a minimum for composites with 10 vol.% Al_2O_3 and then raising slightly for composites with 25 vol.% Al_2O_3. As stated in Section 3.1, XRD results showed that cristobalite formation was hindered by Al_2O_3 addition and in composites with an Al_2O_3 content $\geqslant$10 vol.% the presence of cristobalite was not detected. The decrease of CET values from G to G-5A to G-10A is related to cristobalite suppression, while the increase for G-25A is related to the presence of a larger amount of alumina, which has a CET of 5.5–7.1 [19,20], higher than that of the borosilicate glass (Table 1). CET for G samples sintered at 1000 °C was lower than for G samples sintered at 800 °C, suggesting that samples sintered at 800 °C contained a higher amount of cristobalite. This in agreement with the results obtained in a previous work performed by some of the present authors [30], where the thermal behavior of the monolithic borosilicate glass was studied by different thermal analysis techniques and XRD, and where it was found that the maximum crystallization of the glass occurred in the temperature range 780–800 °C. CET values for the different composites (G-5A, G-10A and G-25A) sintered at 800 and 1000 °C are rather similar, although as shown in Figs. 1 and 2, denser samples were obtained after sintering at 1000 °C. As reported by Coble and Kingery [45], the effect of porosity on the CET may be neglected when the samples have a relative density above 85%, as it is in the present case.

Table 4
Coefficient of thermal expansion of the sintered composite samples, $\alpha_{l(25-200°C)}$ (°C^{-1}).

Sample	Sintering temperature (°C)	
	800	1000
G	9.8×10^{-6}	6.7×10^{-6}
G-5A	5.9×10^{-6}	5.8×10^{-6}
G-10A	4.7×10^{-6}	4.6×10^{-6}
G-25A	5.2×10^{-6}	5.0×10^{-6}

3.3. Electric and dielectric properties of the composites

Under normal temperatures borosilicate glass is non-conductive and acts as an insulator. Specific electric resistance of a monolithic borosilicate glass sample at room temperature (20 °C) and in a humidity-free environment is in the range 10^{11}–10^{13} Ω m [4].

Electrical conductivity measurements for all composite samples revealed that dc conductivity (σ_{dc}) increases with the rise of the sample temperature and alumina content (Fig. 6 and Table 5) indicating an increase in the number of Al^{3+} ions present in the borosilicate glass structure as network modifiers.

The dc conductivity of G samples (borosilicate glass without alumina addition) is higher when sintered at 1000 °C than at 800 °C (Table 5), because at 1000 °C there is a denser structure (Fig. 1) and therefore a higher number of charge carriers. The rise of dc activation energy ($E_{a(dc)}$), achieved through the slope of the $\ln(\sigma_{dc})$ vs. $1/T$ plot (Eq. (1)), with the rise of the sintering temperature, from 800 to 1000 °C (Table 5), indicates that the sintering process gives origin to a structural modification that leads to an increase in the amount of charge carriers. These structural differences are evident when we analyse the ac conductivities of G samples treated at different temperatures (Table 5). The ac conductivity of G samples sintered at 800 °C is higher than that of G samples sintered at 1000 °C indicating the existence, in the 800 °C treated samples, of a higher number of dipoles that can follow the external electric field. However, from the dc results (Table 5), an increase in the number of network modifiers in G samples sintered at 1000 °C can be assumed. Thus, the obtained results suggest that in G samples sintered at 1000 °C the contribution of the mobile ions to the dielectric response decreases. In G sample, sintered at 1000 °C, the value of ε (approximately 5, Table 5) is close to that of a borosilicate glass, which is approximately 4.8 at 1 MHz [7]. The precipitation of cristobalite should not increase the dielectric constant of sintered G sample because the dielectric constant of cristobalite itself is 3.8 at 1 MHz [25]. The decrease of ε, in G samples, with the rise of sintering temperature can be related to the increase in the number of network modifiers. In fact, the increase in the glass structure densification (Fig. 1) leads to a decrease in the average distance between the dipoles formed by the modifier ions. Thus, the presence of cooperative phenomenon between these dipoles can justify the observed decrease of the dipole moment [32,34,46]. This phenomenon becomes more evident in denser structures.

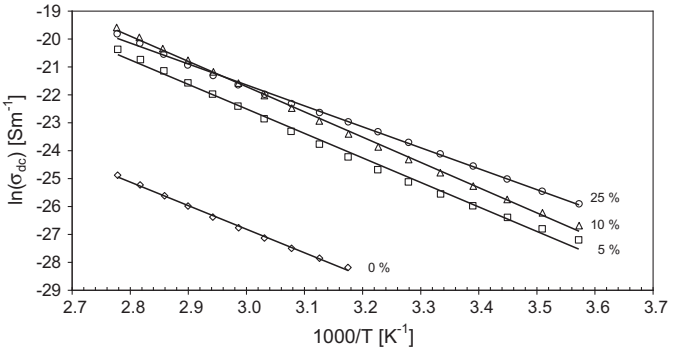

Fig. 6. $\ln(\sigma_{dc})$ vs. $1000/T$ spectra (the line presents the theoretical fit) of the samples sintered at 800 °C (Al_2O_3 content in the composites is indicated).

Table 5
The dc conductivity (σ_{dc}) at 300 K, the dc activation energy ($E_{a(dc)}$), the ac conductivity (σ_{ac}), the dielectric constant (ε) and the loss tangent ($\tan\delta$) at 1 kHz and 300 K, with the correspondent statistic errors.

Sintering temperature (°C)	Al_2O_3 content (vol.%)	σ_{dc} ($\times 10^{-13}$ S m^{-1})	$E_{a(dc)}$ (kJ/mol)	σ_{ac} ($\times 10^{-10}$ S m^{-1})	ε	$\tan\delta$ ($\times 10^{-2}$)
800	0	2.33 ± 0.03	70.19 ± 1.24	66.08 ± 0.74	5.43 ± 0.06	2.19 ± 0.03
	5	79.78 ± 0.63	73.01 ± 1.33	63.92 ± 0.51	6.49 ± 0.05	1.77 ± 0.02
	10	170.69 ± 1.54	75.27 ± 0.75	66.27 ± 0.60	6.24 ± 0.06	1.91 ± 0.02
	25	334.58 ± 4.56	62.45 ± 0.61	75.05 ± 2.98	6.90 ± 0.09	1.95 ± 0.08
1000	0	3.68 ± 0.04	76.69 ± 1.19	41.69 ± 0.85	5.08 ± 0.05	1.47 ± 0.03
	5	91.09 ± 0.93	76.53 ± 1.26	70.57 ± 0.73	5.96 ± 0.06	2.13 ± 0.03
	10	110.07 ± 1.12	77.03 ± 1.01	76.98 ± 0.79	6.68 ± 0.07	2.03 ± 0.03
	25	198.06 ± 1.15	75.82 ± 1.27	77.30 ± 0.96	7.21 ± 0.08	1.93 ± 0.03

The dc conductivity of G-5A composite samples, sintered at 800 and 1000 °C, is higher than that of G samples sintered under the same conditions because some Al^{3+} ions are diffused from the alumina structure into the glass structure, where they are inserted as network modifiers. Also, the amount of Al^{3+} ions diffused into the glass structure is higher at 1000 °C than at 800 °C. G-5A sample sintered at 800 °C presents an ac conductivity value of 63.92×10^{-10} S m^{-1}, while if sintered at 1000 °C has a value of 70.57×10^{-10} S m^{-1} (Table 5). This difference is attributed to the amount of Al^{3+} ions inserted in the glass structure as modifiers and formers. The excess of negative charge created by the network former Al^{3+} ions, inserted in tetrahedral sites, is compensated by the Na^+, K^+ or Al^{3+} ions inserted in the glass network as modifiers [47]. This situation causes an increase in the number of dipoles. Nevertheless, the dc activation energy ($E_{a(dc)}$) (Eq. (1)) is higher in the case of the 1000 °C sample than is the 800 °C (Table 5) because the two glasses have different structures, as in the case of G samples sintered at 800 and 1000 °C. However, the ε values of these samples have an opposite behavior. Thus, it is suggested that the applied electric field has not enough influence in the orientation of the dipoles.

The borosilicate glass/alumina composites with 10 and 25 vol.% of alumina, G-10A and G-25A, respectively, have higher values of dc conductivity than G-5A samples. This is justified by the increase of Al^{3+} ion flux into the borosilicate glass structure. In spite of that, the dc conductivity values of samples treated at 800 °C are higher than those of samples treated at 1000 °C. This behavior can be related with the incapacity of borosilicate glass structure to support the insertion of an excess of Al^{3+} ions. Thus, in the case of samples sintered at 1000 °C, the borosilicate glass structure segregates part of the Al^{3+} ions as Al_2O_3. As in the case of G-5A samples, G-10A and G-25A samples have higher σ_{ac} and ε values due to the amount of Al^{3+} ions present in the glass structure as formers and modifiers and to the amount of alumina in the composite, respectively.

Fig. 7 shows the frequency dependence of ε, measured at room temperature, for the composites with various volume fractions of filler sintered at 1000 °C. It can be observed that ε increases with the increase of the Al_2O_3 content and it decreases with the rise of the frequency, as expected. The value of ε for Al_2O_3 is 9.8 at 1 MHz [7], higher than ε for borosilicate glass and for cristoblite at 1 MHz, which is 4.8 [7] and 3.8 [25], respectively. From Fig. 7 there is no evidence for the existence of dielectric relaxation mechanisms in the measuring frequency range.

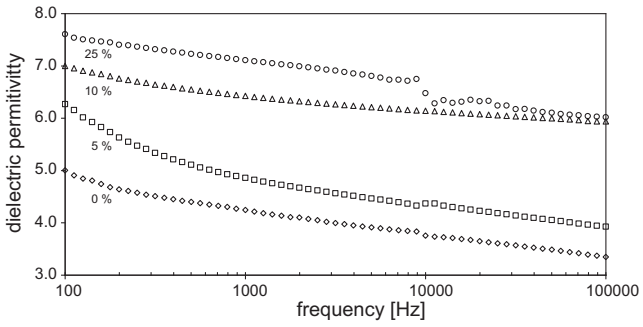

Fig. 7. Frequency dependence of the dielectric constant, measured at room temperature, for the samples sintered at 1000 °C (Al_2O_3 content in the composites is indicated).

Considering that ε values, for commercial low temperature co-fired ceramics and composites (LTCCs), which are commonly measured at low frequencies, are in the range of 3–10 [16], it is observed that ε values measured for the produced composites (5–7.2) are within such range. Furthermore, it should be noted that the values of the dissipation factor tanδ of the composites borosilicate glass–alumina is similar and quite low (i.e. of the order of 10^{-2}). This indicates that all these materials are both good insulators as well as they have low dielectric heating properties.

4. Conclusions

The densification of borosilicate-glass matrix composites, containing up to 25 vol.% alumina and sintered at 800 and 1000 °C was due to viscous flow. Cristobalite was formed in some sintered samples, but it was undetected in samples containing an amount of filler $\geqslant$10 vol.%. The addition of Al_2O_3 particles hinders the formation of cristobalite, because during the sintering process some Al^{3+} ions are diffused into the glass, with a strong coupling between Al^{3+} from Al_2O_3 and Na^+ from the borosilicate glass that leads to changes in glass structure and composition. These structural changes were also responsible for the electrical behavior of the samples. The dc conductivity of all samples increased with sample temperature and Al_2O_3content. The composite samples exhibited an increase in ac conductivity with the increase in the amount of Al^{3+} ions present in the glass structure as formers and modifiers. An increase in dielectric constant values was observed with the increase in the Al_2O_3content present in the composites. The rise of the structure densification, for the samples without the addition of Al_2O_3, leads to a decrease in their dielectric constant and an increase in their dc conductivity.

The critical Al_2O_3content for the present composites, processed from a borosilicate glass and a 2 μm mean particle size Al_2O_3 powder and sintered at 800 and 1000 °C, was found to be 10 vol.%. The resulting cristobalite-free borosilicate glass–alumina composite has a coefficient of thermal expansion of $\sim 4.6 \times 10^{-6}$ °C^{-1} in the temperature range 25–200 °C, a dielectric constant of 6–6.5 at 1 kHz and it is a good electrical insulator.

Acknowledgement

The authors acknowledge financial support given by Fundação para a Ciência e a Tecnologia (Portugal) to I3N and CICECO.

References

[1] J.H. Park, S.J. Lee, Mechanism of preventing crystallization in low-firing glass/ceramic composites substrates, J. Am. Ceram. Soc. 78 (1995) 1128–1130.
[2] Z. Wang, Y. Hu, H. Lu, F. Yu, Dielectric properties and crystalline characteristics of borosilicate glasses, J. Non-Cryst. Solids 354 (2008) 1128–1132.
[3] N. Santha, S. Shamsudeen, N.T. Karunakaran, J.I. Naseemabeevi, Spectroscopic, dielectric and optical properties of $60ZnO–30B_2O_3–10SiO_2$ glass–Al_2O_3 composites, Int. J. Appl. Ceram. Technol. 8 (2011) 1042–1049.
[4] A.R. Boccaccini, B.J.C. Thomas, G. Brusatin, P. Colombo, Mechanical and electrical properties of hot-pressed borosilicate glass matrix composites containing multi-wall carbon nanotubes, J. Mater. Sci. 42 (2007) 2030–2036.
[5] A.A. El-Kheshen, M.F. Zawrah, Sinterability, microstructure and properties of glass/ceramic composites, Ceram Int. 29 (2003) 251–257.
[6] M.F. Zwarah, E.M.A. Hamzawy, Effect of cristobalite formation on sinterability, microstructure and properties of glass/ceramic composites, Ceram. Int. 28 (2002) 123–130.
[7] A.A. El-Kheshen, M.F. Zawrah, M. Awaad, Densification, phase composition, and properties of borosilicate glass composites containing nano-alumina and titania, J. Mater. Sci: Mater. Electron. 20 (2009) 637–643.
[8] K. Nakashima, K. Noda, K. Mori, Time-temperature-transformation diagrams for borosilicate glasses and preparation of chemically durable porous glasses, J. Am. Ceram. Soc. 80 (1997) 1101–1110.
[9] A.R. Boccaccini, Special review, launching into the great new millennium, glass and glass–ceramic matrix composites materials, J. Ceram. Soc. Jpn. 109 (2001) S99–S109.
[10] M. Kotoul, J. Pokluda, P. Sandera, I. Dlouhy, Z. Chlup, A.R. Boccacini, Toughening effects quantification in glass matrix composite reinforced by alumina platelets, Acta Mater. 56 (2008) 2908–2918.
[11] I. Dlouhy, A.R. Boccacini, Preparation, microstructure and mechanical properties of metal-particulate/glass-matrix composites, Composites Sci. Technol. 56 (1996) 1415–1424.
[12] A.R. Boccacini, D.R. Acevedo, G. Brusatin, P. Colombo, Borosilicate glass matrix composites containing multi-wall carbon nanotubes, J. Eur. Ceram. Soc. 25 (2005) 1515–1523.
[13] E. Bernardo, E. Stoll, A.R. Boccaccini, Novel basalt fibre reinforced glass matrix composites, J. Mat. Sci. 41 (2006) 1207–1211.
[14] V. Cannillo, T. Manfredini, M. Montorsi, A.R. Boccaccini, Investigation of the mechanical properties of Mo-reinforced glass-matrix composites, J. Non-Cryst. Solids 344 (2004) 88–93.
[15] R.R. Tummala, Ceramic and glass–ceramic packaging in the, J. Am. Ceram. Soc. 74 (1991) (1990) 895–908.
[16] H. Jantunen, T. Kangasvieri, J. Vahakangas, S. Leppavuori, Design aspects of microwave components with LTCC technique, J. Eur. Ceram. Soc. 23 (2003) 2541–2548.
[17] G.H. Chen, L.J. Tang, J. Cheng, M.H. Jiang, Synthesis and characterization of CBS glass/ceramic composites for LTCC application, J. Alloy Compd. 478 (2009) 858–862.
[18] C.C. Chiang, S.F. Wang, Y.R. Wang, Y.F. Hsu, Characterization of $CaO-B_2O_3-SiO_2$ glass–ceramics, Thermal and electrical properties, J. Alloy Compd. 461 (2008) 612–616.
[19] S. Wu, L.C. De Jonghe, V.B. Dutta, Dielectric ceramics: processing, properties and application, in: K.M. Nair, J.P. Guha, A. Okamoto (Eds.), Ceramics Transactions 32, Am. Ceram. Soc, Ohio, 1993, pp. 299–308.
[20] C.R.M. Grovenor, Microelectronic Materials, IOP Publishing Ltd., 1998, p. 328.
[21] A. Stiegelschmitt, A. Roosen, C. Ziegler, S. Martius, L.P. Schmidt, Dielectric data of ceramic substrates at high frequencies, J. Eur. Ceram. Soc. 24 (2004) 1463–1466.
[22] J.H. Jean, T.K. Gupta, Effect of alumina on densification of binary borosilicate glass composite, J. Mater. Res. 9 (1994) 1990–1996.
[23] J.M. Wu, H.L. Huang, Microwave properties of zinc, barium and lead borosilicate glasses, J. Non-Cryst. Solids 260 (1999) 116–124.
[24] V.A. Greenhut, Adhesives and sealants, in: H.F. Brinson (Ed.), Engineered materials handbook 4, ASM International, Materials Park, OH, 1991, pp. 298–311.
[25] E.E. Hamzawy, A.A. El-Kheshen, M.F. Zawrah, Densification and properties of glass/cordierite composites, Ceram. Int. 31 (2005) 383–389.
[26] J.H. Jean, T.K. Gupta, Devitrification inhibitor in binary borosilicate glass composite, J. Mater. Res. 8 (1993) 356–363.
[27] M.M.R.A. Lima, R.C.C. Monteiro, Crystallization of a borosilicate glass during sintering studied by dilatometry and XRD analysis, Mater. Sci. Forum 455–456 (2004) 212–215.
[28] R.C.C. Monteiro, M.M.R.A. Lima, Effect of compaction on the sintering of borosilicate glass–alumina composites, J. Eur. Cer. Soc. 23 (2003) 1813–1818.
[29] M.M.R.A. Lima, Sintering and Crystallization of a Borosilicate Glass – Effect of Alumina Addition, Ph. D. Thesis (in Portuguese), New University of Lisbon, 2003.
[30] M.M. Lima, R. Monteiro, Characterization and thermal behaviour of a borosilicate glass, Thermochim. Acta 373 (2001) 69–74.
[31] M.P. Graça, M.A. Valente, M.G. Ferreira da Silva, Electrical properties of lithium niobium silicate glasses, J. Non-Cryst. Solids 325 (2003) 267–274.
[32] F. Kremer, A. Schönhals, Broadband Dielectric Spectroscopy, Springer, Germany, 2002.
[33] A.K. Jonsher, Dielectric relaxation in solids, VCH, London, 1983.
[34] J.R. Macdonald, Impedance Spectroscopy, John Wiley and Sons, New York, 1987.
[35] M.P.F. Graça, M.G. Ferreira da Silva, A.S.B. Sombra, M.A. Valente, Study of the electric and dielectric properties of $SiO_2–Li_2O–Nb_2O_5$ sol–gel glass–ceramics, J. Non-Cryst. Solids 352 (2006) 1501–1505.
[36] M.N. Rahaman, L.C. De Jonghe, G.W. Scherer, R.J. Brook, Creep and densification during sintering of glass powder compacts, J. Am. Ceram. Soc. 70 (1987) 766–774.
[37] M.N. Rahaman, L.C. De Jonghe, Effect of rigid inclusions on the sintering of glass powder compacts, J. Am. Ceram. Soc. 70 (1987) C348–C351.
[38] J.H. Jean, T.K. Gupta, Liquid-phase sintering in the glass-cordierite system, J. Mater. Sci. 27 (1992) 1575–1584.
[39] M. Eberstein, S. Reinsch, R. Muller, J. Deubener, W.A. Schiller, Sintering of glass matrix composites with small rigid inclusions, J. Eur. Ceram. Soc. 29 (2009) 2469–2479.
[40] J.H. Jean, T.K. Gupta, Crystallization kinetics of binary borosilicate glass composite, J. Mater. Res. 7 (1992) 3103–3111.
[41] J.H. Jean, T.K. Gupta, Alumina as a devitrification inhibitor during sintering of borosilicate glass powders, J. Am. Ceram. Soc. 76 (1993) 2006–2010.
[42] J.H. Jean, T.K. Gupta, Devitrification inhibitor in borosilicate glass and binary borosilicate glass composite, J. Mater. Res. 10 (1995) 1312–1320.
[43] J.H. Jean, C.R. Chang, R.L. Chang, T.H. Kuan, Effect of alumina particle size on prevention of crystal growth in low-k silica dielectric composite, Mater. Chem. Phys. 40 (1995) 50–55.
[44] J.I. Goldstein, D.B. Williams, G. Cliff, Quantitative X-ray analysis, in: D.C. Joy, A.D. Romig, J.I. Goldstein (Eds.), Principles of Analytical Electron Microscopy, Plenum Press, New York and London, 1986, p. 155.
[45] R.L. Coble, W.D. Kingery, Effect of porosity on physical properties of sintered alumina, J. Am. Ceram. Soc. 39 (2006) 377–385.
[46] G. Bitton, Y. Feldman, A.J. Agranat, Relaxation processes of off-center impurities in KTN:Li crystals, J. Non-Cryst. Solids 305 (2002) 362–367.
[47] M.G. Ferreira da Silva, Study of the structural insertion of Al^{3+} in the $Al_2O_3–SiO_2$ and $Nd_2O_3–Al_2O_3–SiO_2$ glass systems, J. Non-Cryst. Solids 352 (2006) 807–820.